Am J Transl Res 2025;17(5):4023-4037
www.ajtr.org /ISSN:1943-8141/AJTR0163878

Original Article

Metabolic pathways in anal fistula: paving the way for innovative treatments

Minjie Wang[1], Yibin Pan[1], Xi Zhang[1], Chen Pan[2], Yongqing Cao[1]

[1]Department of Anal and Intestinal Disease, Longhua Hospital, Shanghai University of Traditional Chinese Medicine, Shanghai 200030, China; [2]Department of General Surgery, The First Affiliated Hospital of USTC, Division of Life Sciences and Medicine, University of Science and Technology of China, Hefei 230001, Anhui, China

Received February 12, 2025; Accepted April 9, 2025; Epub May 15, 2025; Published May 30, 2025

Abstract: Background: Anal fistula, particularly in its cryptoglandular form, is a common yet challenging condition to treat, often resulting in poor healing and recurrent infections. Investigating the metabolic changes associated with anal fistula may offer valuable insights into its underlying mechanisms and assist in the development of more effective treatments. Methods: This study conducted a comprehensive analysis of serum samples from patients with various types of anal fistula and healthy controls. Metabolomic profiling was performed to identify differences in metabolic pathways between the groups. Results: The analysis revealed significant metabolic alterations in patients with anal fistula, particularly in fatty acid metabolism, sphingolipid metabolism, and amino acid metabolism. Notably, metabolites such as adrenic acid, LysoPC (22:5n6), and PC (18:0/22:4) were significantly associated with the progression of anal fistula. These metabolites could serve as biomarkers for the condition, with particular relevance in differentiating between acute and chronic stages. Conclusion: The study provides new insight into the metabolic basis of anal fistula, identifying specific metabolic pathways and metabolites that may play crucial roles in its progression. These findings may contribute to the development of targeted therapies for more effective treatment.

Keywords: Anal fistula, metabolomics, fatty acid metabolism, sphingolipid metabolism, biomarkers

Introduction

Anal fistula is a common surgical condition that presents significant challenge for both patients and healthcare providers. The complexity of anal fistulas often stems from their intricate anatomy and the risk of recurrence, which complicates treatment. Various surgical techniques have been developed to address these challenges, each with its own advantages and limitations.

Preserving the anal sphincter to prevent incontinence is a crucial consideration in the management of complex anal fistulas. Sphincter-sparing techniques, such as the Video-Assisted Anal Fistula Treatment (VAAFT), have emerged as minimally invasive alternatives aimed at addressing fistulas while preserving sphincter function. VAAFT employs a fistuloscope to visualize the fistula tract and perform necessary surgical procedures under direct vision. This technique has demonstrated encouraging outcomes in terms of healing rates and patient satisfaction [1].

Stem cell therapy has emerged as a novel treatment modality for complex anal fistulas, particularly those associated with Crohn's disease. Adipose-derived stem cells have demonstrated promise in promoting healing and reducing recurrence rates, offering a sphincter-preserving alternative to traditional surgical methods [2]. Meta-analyses have supported the efficacy and safety of mesenchymal stem cell therapy, underscoring its role in the management of complex perianal fistulas [3]. The use of fistula plugs offers another sphincter-sparing option. These bioprosthetic plugs are designed to obstruct the fistula tract and facilitate healing. Research has demonstrated the effectiveness of fistula plugs in managing complex anal fistulas, with success rates varying depending on the type of plug used and the unique characteristics of the fistula [4].

https://doi.org/10.62347/UWZM3553

The development of anal fistulas often follows the formation of perianal abscesses, which are characterized by an inflammatory process that can lead to tissue destruction [5]. The immune response plays a critical role in this process, with various immune cells and cytokines contributing to the pathogenesis of both perianal abscesses and anal fistulas. Inflammatory bowel diseases, such as Crohn's disease, are known to exacerbate these conditions through their influence on the intestinal immune system [6]. A key factor in the development of anal fistulas is the role of cytokines, particularly interleukin-17 (IL-17). Studies have shown that IL-17 levels are significantly elevated in the tissues and peripheral blood of patients with perianal abscesses and anal fistulas, suggesting its involvement in the inflammatory process and progression of these conditions [7]. The association between IL-17 levels and abscess severity, as well as the propensity for fistula formation, suggests that therapeutically targeting this cytokine may be a viable strategy. Furthermore, the gut microbiota plays a significant role in the progression of perianal abscesses and fistulas. Alterations in gut microbiota composition have been identified in individuals with perianal abscesses, with specific bacteria possibly serving as diagnostic biomarkers [8]. These microbial changes can influence the immune response, further contributing to the pathogenesis of anal fistulas. Additionally, tumor necrosis factor (TNF) has been implicated in the pathogenesis of Crohn's disease-associated fistulas. TNF is strongly expressed in the transitional cells of Crohn's disease fistulas, supporting an involvement of epithelial-mesenchymal transition (EMT) in their development [9]. This suggests that TNF inhibitors might be effective in managing fistulas associated with Crohn's disease, although their efficacy may be limited in cases without luminal inflammation [10]. The role of the immune system in the development of anal fistulas is further reinforced by the presence of diverse immune cells, including T cells and macrophages, within the affected tissues. These cells, along with cytokines such as IL-6 and TNF-α, contribute to the chronic inflammation characteristic of anal fistulas [11]. The pathogenesis of anal fistula involves a complex interplay of cellular signaling pathways, multiple cytokines, growth factors, and interleukins during the wound healing cascade, in response to a chronic, infectious nonhealing wound caused by ruptured perianal abscess. Dysregulated healing following the development of an anal fistula can ultimately lead to its re-formation.

This study presents a novel approach by utilizing metabolomic profiling to uncover the underlying metabolic changes associated with anal fistula. Unlike previous studies that have primarily focused on surgical and immunological aspects, our research delves into the metabolic alterations that occur in patients with anal fistula, providing a new perspective on the disease's pathogenesis. By identifying key metabolites, such as adrenic acid, LysoPC (22:5n6), and PC (18:0/22:4), we propose potential biomarkers that could revolutionize the diagnosis and monitoring of anal fistula. These biomarkers could enable earlier detection and more personalized treatment strategies, possibly improving patient outcome.

Materials and methods

Inclusion and exclusion criteria of subjects

The inclusion criteria for the anal fistula cohort were established based on the 2016 *Clinical Practice Guidelines for Anorectal Abscess, Fistula-in-Ano, and Rectovaginal Fistula Management* (American Society of Colon and Rectal Surgeons) [12]. Disease classification was based on infectious status: acute anal fistula (concurrent perianal abscess or local infection at fistula onset) versus simple anal fistula (absence of concomitant infections). To qualify for inclusion, patients were required to: (1) provide blood samples as protocol-specified: Blood samples were collected during routine clinical visits. Serum was separated by centrifugation at 3000 rpm for 10 minutes and stored at -80°C until further analysis; (2) submit complete medical documentation: Patients were required to provide detailed medical histories, including previous treatments, comorbidities, and any history of inflammatory bowel disease (IBD) or other gastrointestinal disorders; (3) The study protocol was approved by the Institutional Review Board of Shanghai University of Traditional Chinese Medicine (Approval No. 2020LCSY032) in compliance with Helsinki Declaration standards.

Inclusion criteria for healthy controls: (1) no perianal abscesses, anal fistulas, or systemic

discomfort symptoms; (2) no history of chronic metabolic disorders, gastrointestinal organic lesions, or cardiovascular/cerebrovascular diseases; and (3) unremarkable physical examination findings.

Exclusion criteria: (1) age <18 years; (2) severe cardiopulmonary dysfunction (NYHA class III-IV or GOLD stage 3-4); (3) hepatic insufficiency (Child-Pugh B/C) or renal impairment (eGFR <30 mL/min/1.73 m^2); (4) thyroid disorders, diabetes mellitus, or gastrointestinal malignancies; (5) active infections (tuberculosis, HIV infection, or syphilis); (6) necrotizing fasciitis; (7) inflammatory bowel disease; (8) trauma-induced perianal pathologies; and (9) pregnancy or puerperium status.

Serum samples were collected from 12 patients with acute anal fistula, 20 patients with simple anal fistula, and 20 healthy controls. The samples were processed and stored according to standardized protocols to ensure consistency and reliability in the metabolomic analysis.

Sample pretreatment by liquid chromatography

The serum samples were prepared following a meticulous procedure. Initially, the sub-packaged serum was thawed at 4°C and then gently mixed using a liquid transfer gun to ensure even distribution. Subsequently, 100 μL of serum was carefully transferred into 2 mL EP tubes, and 400 μL of methanol solution was added, followed by thorough mixing on a vortex oscillator for 3 minutes. Subsequently, 900 μL of methyl tert-butyl ether and 250 μL of ultrapure water were added, and the mixture was further homogenized on the vortex oscillator for an additional 3 minutes. The resulting mixture was then placed on a rolling shaker for 10 minutes, followed by a 10-minute incubation at room temperature to allow for natural stratification. Subsequently, the mixture underwent high-speed, low-temperature centrifugation at 4°C and 13,000 g for 10 minutes. The lipids extract (700 μL) and polar small molecule extract (400 μL) were carefully transferred into another set of EP tubes. All remaining samples were thoroughly mixed and centrifuged under the same conditions as before. From the upper and lower layers, 700 μL of lipids extract and 400 μL of polar small molecule extract were collected as quality control (QC) samples for lipids and polar small molecular metabolites, respectively. Lastly, all samples, including QC samples, underwent vacuum freeze-drying before being re-dissolved in sample compound solutions prior to analysis. Polar small molecular metabolites were reconstituted in acetonitrile-water (1:3, v/v), while lipids were reconstituted in acetonitrile-isopropanol (1:1, v/v) for subsequent analysis.

Liquid chromatography-mass spectrometry analysis

We employed an UltiMate 3000 ultra-high-performance liquid chromatograph coupled with a Q-Exactive quadrupole orbitrap high-resolution mass spectrometer for comprehensive analysis of polar metabolites and lipids. For polar metabolite analysis, reversed-phase chromatography was used, and both positive and negative ions were detected. For positive ion detection, an Excel2 C18-PFP column (ACE Co., UK, 3.0 μm, 2.1 × 100 mm) was used with a linear gradient elution. The mobile phase consisted of 0.1% formic acid in water (A) and acetonitrile (B). The elution gradient initiated at 2% at 0 minutes and gradually reached 98% over the course of 10 minutes. For negative ion detection, an Acquity HSS C18 column (Waters Co., 1.8 μm, 2.1 × 100 mm) was utilized, with the mobile phase comprising water (A) and acetonitrile/methanol (B), both containing ammonium bicarbonate buffer salt. The elution gradient initiated at 0 minutes, with the B mobile phase at 2%, linearly increasing to 100% over the subsequent 10 minutes, followed by a 5-minute flush of the chromatographic column. The flow rate, injection volume, and column temperature were maintained at 0.4 mL/μL, 5 μL, and 50°C, respectively.

For lipids analysis, simultaneous positive and negative ion chromatographic separation was executed using an Accucore C30 column (Thermo Science, 2.6 μm, 2.1 × 100 mm). The mobile phase consisted of 60% acetonitrile-water (A) and 10% acetonitrile-isopropanol (B), both supplemented with 10 mmol/L ammonium formate and 0.1% formic acid (FA). The elution gradient commenced at 10% for phase B at 0 minute, gradually increasing to 50% over 5 minutes, further progressing to 100% within 23 minutes. The remaining 7 minutes were used for elution and column equilibrium. The flow

rate was maintained at 0.3 mL/min, and the separation temperature was maintained at 50°C.

Mass spectrometry detection parameters

The Q-Orbitrap mass spectrometer was used with identical ionization parameters for both polar metabolites and lipids. These parameters included a sheath gas flow of 45 arb, auxiliary gas at 10 arb, heating temperature set to 355°C, capillary temperature at 320°C, and an S lens radio frequency level of 55%. For comprehensive analysis, the metabolic group extract underwent full scan mode analysis, with a resolution of 700 pm, automatic gain control (AGC) set to 1E6, and a maximum injection time of 200 ms, covering a scan range from 70 to 2000 m/z. Furthermore, a resolution setting of 17,500 was employed for full MS/MS data acquisition, accompanied by a maximum injection time of 80 ms. Collision-induced dissociation, employing nitrogen as the pyrolysis gas, was utilized for metabolite dissociation during analysis.

Data processing and statistical analysis

Upon obtaining the original peak list, data processing was meticulously executed. Redundancies across various detection methods were excluded to ensure the uniqueness of the information. Subsequently, a $\log_2$ transformation was applied to prepare the data for final statistical analysis [13]. Clinical baseline data were expressed as mean ± standard deviation (SD) for continuous variables and as frequencies (percentages) for categorical variables. Statistical analysis was performed using SPSS software (version 25.0, IBM Corp., USA). One-way ANOVA was applied for continuous variables, and the Chi-square test was employed for categorical variables to compare differences between groups [14]. For metabolomic data analysis, multivariate statistical methods, including Principal Component Analysis (PCA), Orthogonal Partial Least Squares Discriminant Analysis (OPLS-DA), and response permutation tests (RPT), were performed using SIMCA-P software (Umetrics, Sweden). The results were visualized with score plots and loading plots to distinguish metabolic profiles between groups. Differential metabolites were identified based on Variable Importance in Projection (VIP) scores >1 and *p*-values <0.05. Univariate analysis of metabolites was conducted using the MetaboAnalyst 6.0 platform (http://www.metaboanalyst.ca) [15, 16]. Results were expressed as fold changes (FC) and *p*-values, with significant metabolites highlighted in volcano and heatmap plots. KEGG pathway analysis was performed to identify enriched metabolic pathways, with results expressed as *p*-values and pathway impact scores. Graphical representations, including pie charts, volcano plots, heatmaps, scatter plots, bar charts, and violin plots, were generated using GraphPad Prism 9.2 (GraphPad Software, USA). Weighted Gene Co-expression Network Analysis (WGCNA) was conducted in R version 4.3.1 (R Core Team, 2023) to identify functional modules associated with anal fistula development [17]. The results were expressed as module-trait relationships and eigengene expression patterns.

Results

Study design

Serum samples were collected from 12 patients with acute anal fistula, 20 patients with simple anal fistula, and 20 healthy controls. The gender distribution was balanced across groups as confirmed by a Chi-square test, with 19 males and 1 female in the healthy control group, 11 males and 1 female in the acute anal fistula group, and 18 males and 2 females in the simple anal fistula group. The participants' ages were closely matched, with mean ages of 32.55±5.53 years for the healthy control group, 33.65±11.36 years for the acute anal fistula group, and 32.25±8.69 years for the anal fistula group. Statistical analysis using one-way ANOVA showed no significant age differences between any two groups ($p>0.05$), ensuring comparability .

To explore the metabolic differences associated with the pathologic changes of anal fistula, we analyzed the metabolites between patients with anal fistula and healthy controls, as well as between patients with acute anal fistula and simple anal fistula. Furthermore, common differential metabolites were identified, and the influence of acute infection on the metabolic changes of anal fistula was minimized by accounting for the baseline state of the condition. Following univariate and multivariate analysis of the identified metabolites, biological annotations and Weighted Gene Co-expression

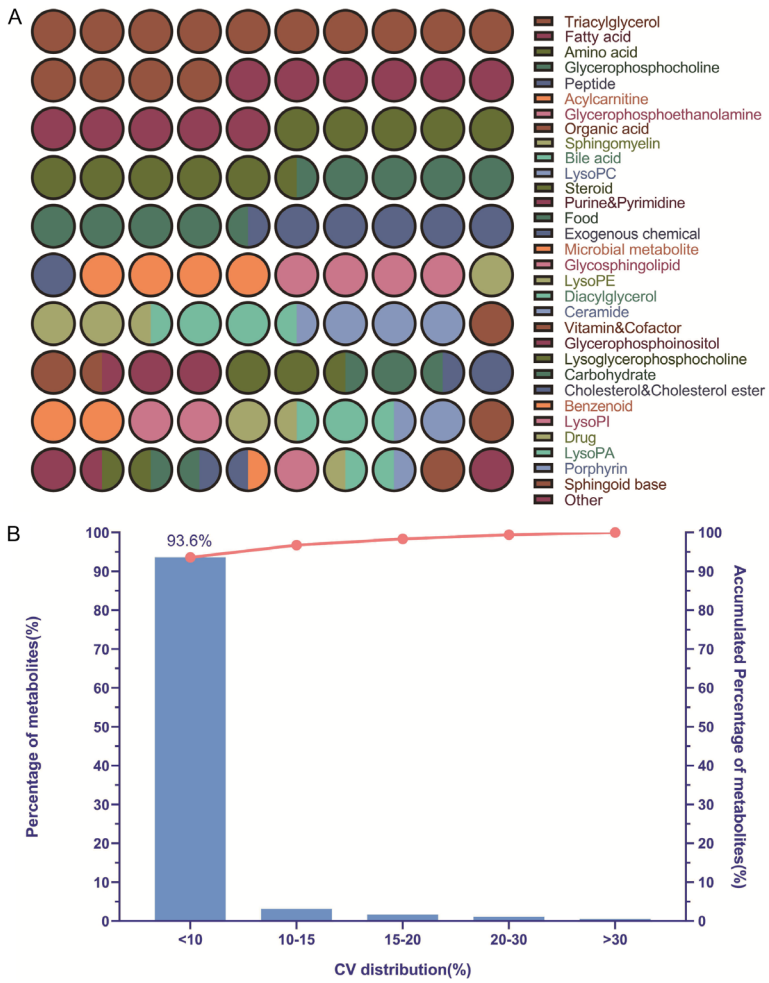

Figure 1. Data quality control. A: Chemical species distribution of the total 1112 metabolites; B: Pareto diagram illustrating the coefficient of variation for metabolites in the QC sample. QC: quality control.

Network Analysis (WGCNA) were used to compare and cluster the annotated serum metabolites.

Metabolite profiles between simple anal fistula and healthy control

To obtain the overall understanding of metabolism in anal fistula, we analyzed polar metabolites and lipids using a non-targeted metabonomic platform (raw data are listed in SupTable). After excluding repetitive and inaccurate compounds in metabonomic analysis, a total of 1112 metabolites were identified (**Figure 1A**). To evaluate data quality and measurement repeatability, we calculated the coefficient of variation (CV or RSD) between QC samples at different stages and visualized the results as a Pareto diagram (**Figure 1B**). A significant proportion (93.6%) of the metabolites exhibit a CV of less than 10%, indicating high detection reliability.

Principal component analysis (PCA) was performed to characterize differential metabolites. The points in the sample plot represent the tested samples, and the distance between them represents the similarities or differences between the samples. The samples were divided into a control (Con) group, Fistula group, and an acute anal fistula group, then a PCA score plot was drawn (**Figure 2A**). The data showed distinct separation among the three groups.

To distinguish between the healthy control group and the simple fistula group, we used Orthogonal Partial Least Squares Discriminant Analysis (OPLS-DA), which revealed a notable separation between these two groups on the score plot (**Figure 2B**). Subsequently, response permutation tests (RPT) were performed to ensure the model's reliability and to confirm an absence of overfitting (**Figure 2C**). Differential metabolites with VIP (Variable Important in Projection) values exceeding 1 and $P<0.05$, as identified by OPLS-DA, were visualized as a volcano plot (**Figure 2D**). The top 25 representative metabolites were selected for heatmap analysis, highlighting significant differences in acylcarnitine, fatty acid, and ceramide between the healthy control and fistula groups (**Figure 2E**). To explore the metabolic implications of these differential metabolites, over-representation analysis (ORA) based on the KEGG database was conducted to assess metabolic pathway enrichment. The results indicated substantial alterations in fatty acid metabolism, particularly unsaturated fatty acid metabolism, and sphingolipid metabolism (**Figure 2F**).

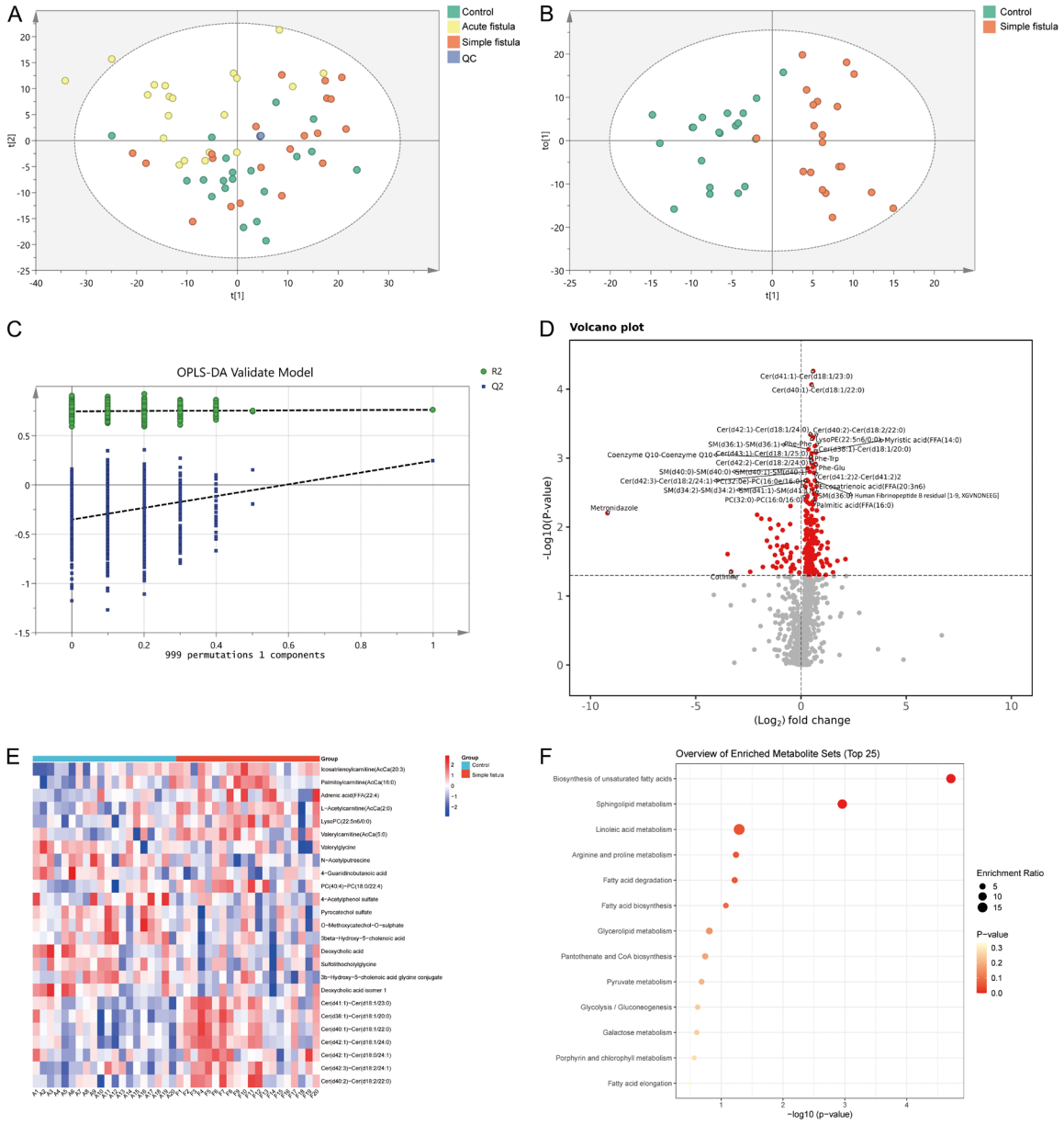

Figure 2. Metabolomic analysis between control group and simple anal fistula group. A: PCA score plot including QC samples and all study samples; B: OPLS-DA score plot distinguishing the healthy control group from the simple fistula group; C: Results of response permutation tests (RPT) of the OPLS-DA model; D: Volcano plot highlighting differential metabolites between the healthy control and fistula groups based on VIP values >1 and P<0.05; E: Heatmap presenting the top 25 differential metabolites; F: KEGG enrichment analysis results depicting altered metabolic pathways in the healthy control and fistula groups. PCA: Principal Component Analysis; OPLS-DA: Orthogonal Partial Least Squares Discriminant Analysis; RPT: Response Permutation Tests; VIP: Variable Importance in Projection; KEGG: Kyoto Encyclopedia of Genes and Genomes.

Metabolite profiles between acute anal fistula and healthy controls

Given the dynamic changes between anal fistula and acute anal fistula, our subsequent analysis aimed to differentiate the healthy control group from the acute anal fistula group. Using OPLS-DA, we observed a distinct separation between these two groups, as depicted in the score plot (**Figure 3A**). To validate the reliability of our model and rule out overfitting, we conducted RPT, and the results are presented in **Figure 3B**. The differential metabolites identified by OPLS-DA with VIP values exceeding 1

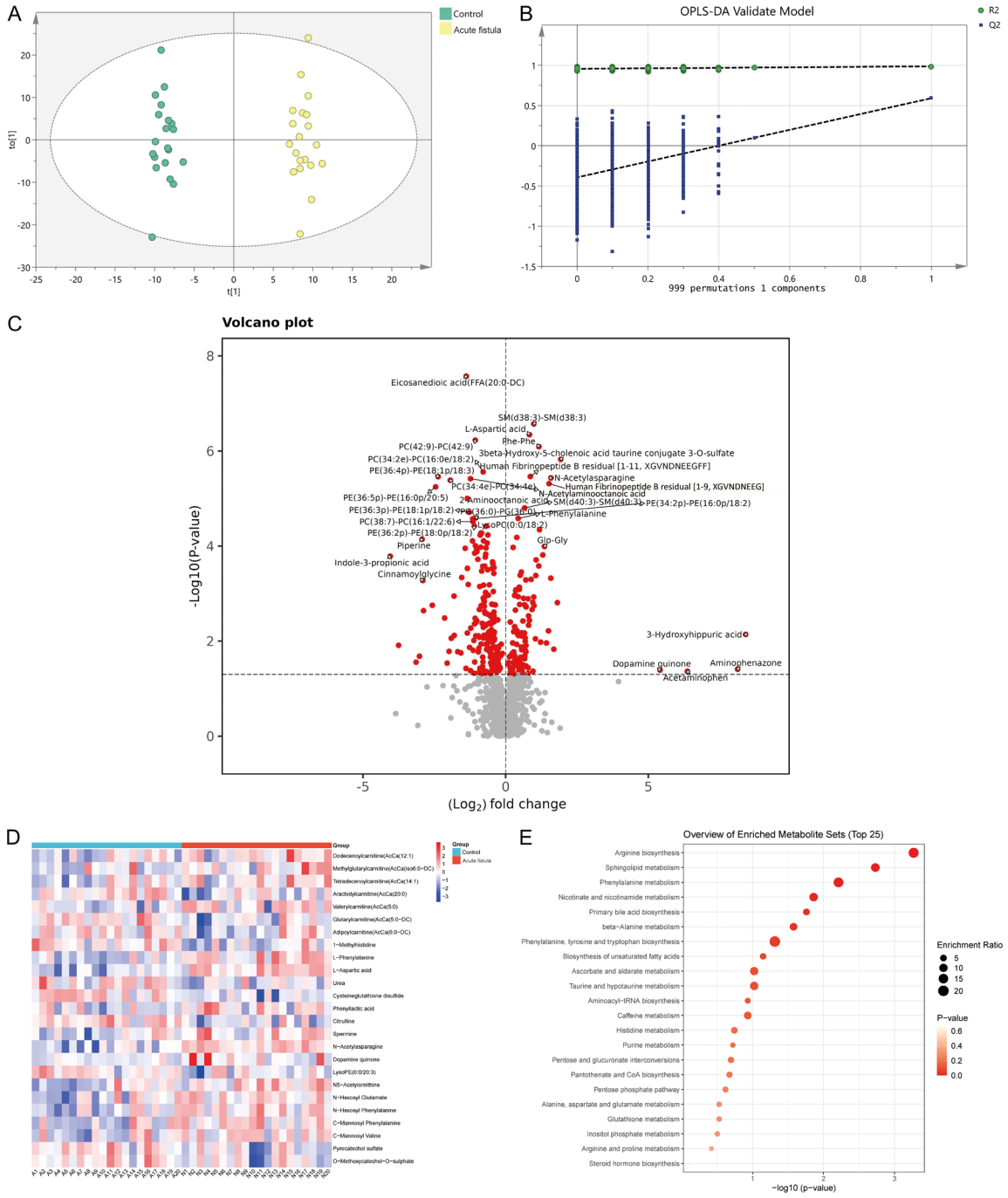

Figure 3. Metabolomic analysis between control group and acute anal fistula group. A: OPLS-DA score plot distinguishing the healthy control group from the acute anal fistula group; B: Results of response permutation tests (RPT) of the OPLS-DA model; C: Volcano plot highlighting differential metabolites between the healthy control and acute anal fistula groups based on VIP values >1 and P<0.05; D: Heatmap representing the top 25 differential metabolites; E: KEGG enrichment analysis results depicting altered metabolic pathways in the healthy control and acute anal fistula groups. OPLS-DA: Orthogonal Partial Least Squares Discriminant Analysis; RPT: Response Permutation Tests; VIP: Variable Importance in Projection; KEGG: Kyoto Encyclopedia of Genes and Genomes.

and P<0.05 were visualized using a volcano plot (**Figure 3C**). For a more detailed overview, we selected the top 25 representative metabolites and analyzed them using a heatmap, which revealed significant variations. In addition to notable differences in acylcarnitine

between the acute fistula group and the healthy control group, alterations in various amino acids were also evident (**Figure 3D**). To better understand the metabolic implications of these differential metabolites, we conducted KEGG metabolic pathway enrichment analysis. The outcomes highlighted substantial modifications in arginine biosynthesis, sphingolipid metabolism, and phenylalanine metabolism (**Figure 3E**).

Metabolite profiles between simple anal fistula and acute anal fistula

The variations observed in species between simple anal fistula and acute anal fistula groups were integrated into subsequent analyses to reduce interference. To differentiate between these subgroups, we employed OPLS-DA, which resulted in a clear distinction between the two groups, as shown in the score plot (**Figure 4A**). To enhance the robustness of our model and mitigate overfitting risks, we performed RPT, with the results illustrated in **Figure 4B**. Subsequently, we visualized the differential metabolites identified by OPLS-DA, focusing on those with VIP values surpassing 1 and *p*-values below 0.05, employing a volcano plot (**Figure 4C**). For a more detailed view, we selected the top 25 representative metabolites and subjected them to heatmap analysis, revealing substantial variances. Particularly notable were the differential metabolites such as LysoPC (lysophosphatidylcholine) and various fatty acids, with a particular emphasis on adrenic acid and the phospholipids containing this free fatty acid (**Figure 4D**). To gain deeper insight into the metabolic implications of these differential metabolites, we conducted KEGG metabolic pathway enrichment analysis. The findings emphasized significant alterations in D-glutamine and D-glutamate metabolism, nitrogen metabolism, and the metabolism of various amino acids (**Figure 4E**).

Continual evaluation of the progression from health to anal fistula development

Previous analyses have revealed significant metabolic differences between the healthy control group and the fistula group, especially during the acute infection phase. In this study, we aim to elucidate the dynamic process from a healthy state to acute anal fistula formation during acute infection, followed by fistula development. By integrating the findings from earlier analyses, we identified specific metabolites that represent the progression of fistula formation, after excluding the influence of acute infection. WGCNA was employed to explore metabolites exhibiting similar trends, and the results demonstrated a lack of significant outlier samples following clustering (**Figure 5A**). We selected a soft threshold of 8 (**Figure 5B**) and obtained the cluster tree for the WGCNA model (**Figure 5C**, **5D**). Among the co-clustered modules, excluding invalid grey modules, we identified 11 modules. Subsequently, Pearson correlation analysis and inter-group trend analysis were performed between modules (**Figure 5E**). Modules with an absolute correlation coefficient exceeding 0.3 were designated as candidate modules. Three candidate modules were identified: pink, turquoise, and yellow, all exhibiting a positive correlation with anal fistula formation and development, with p-values < 0.05 (**Figure 5F**). The pink module primarily featured LysoPC as high-weight metabolism, while the turquoise module predominantly comprised triglyceride (TG) and diglyceride (DG). The yellow module was primarily composed of long-chain free fatty acids. Notably, there was significant overlap between the dynamic modules identified by WGCNA and the significant metabolite differences observed in earlier analyses, providing further validation of our findings.

Next, we conducted a comprehensive analysis by overlaying the differential metabolites identified in the fistula and healthy control groups, with those in the simple acute anal fistula and fistula combined acute anal fistula subgroup. These metabolites were further cross-referenced with the three principal modules from the WGCNA analysis. As a result, seven representative differential metabolites were identified: Adrenic acid, LysoPC (22:5n6), PC (18:0/22:4), Proline betaine, LysoPC (14:0), LysoPC (16:0), and Pyrogallol-1-O-sulphate. Remarkably, adrenic acid displayed a positive association with the development of anal fistula and demonstrated a parallel trend with PC (18:0/22:4), of which it is a constituent.

To provide a clearer illustration of the inter-group variations, violin plots were generated for both adrenic acid and PC (18:0/22:4). Interestingly, adrenic acid levels remained relatively unaffected by acute anal fistula but exhibited a substantial increase in the simple anal

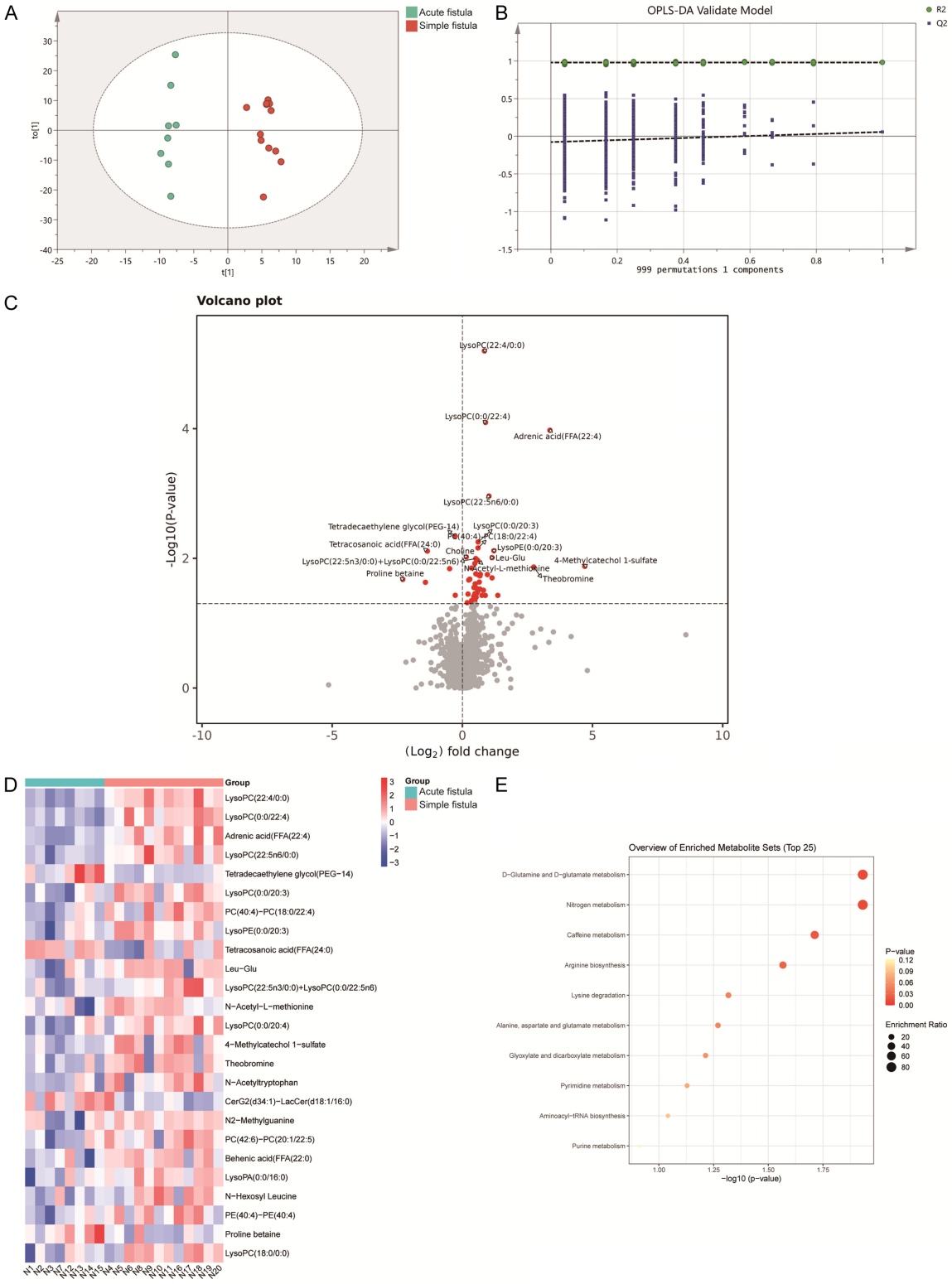

Figure 4. Metabolomic analysis between simple and acute anal fistula group. A: OPLS-DA score plot distinguishing simple anal fistula from acute anal fistula; B: Results of response permutation tests (RPT) of the OPLS-DA model; C: Volcano plot highlighting differential metabolites between simple acute anal fistula and fistula combined with acute anal fistula based on VIP values >1 and P<0.05; D: Heatmap representing the top 25 differential metabolites; E: KEGG enrichment analysis results depicting altered metabolic pathways. OPLS-DA: Orthogonal Partial Least Squares Discriminant Analysis; RPT: Response Permutation Tests; VIP: Variable Importance in Projection; KEGG: Kyoto Encyclopedia of Genes and Genomes.

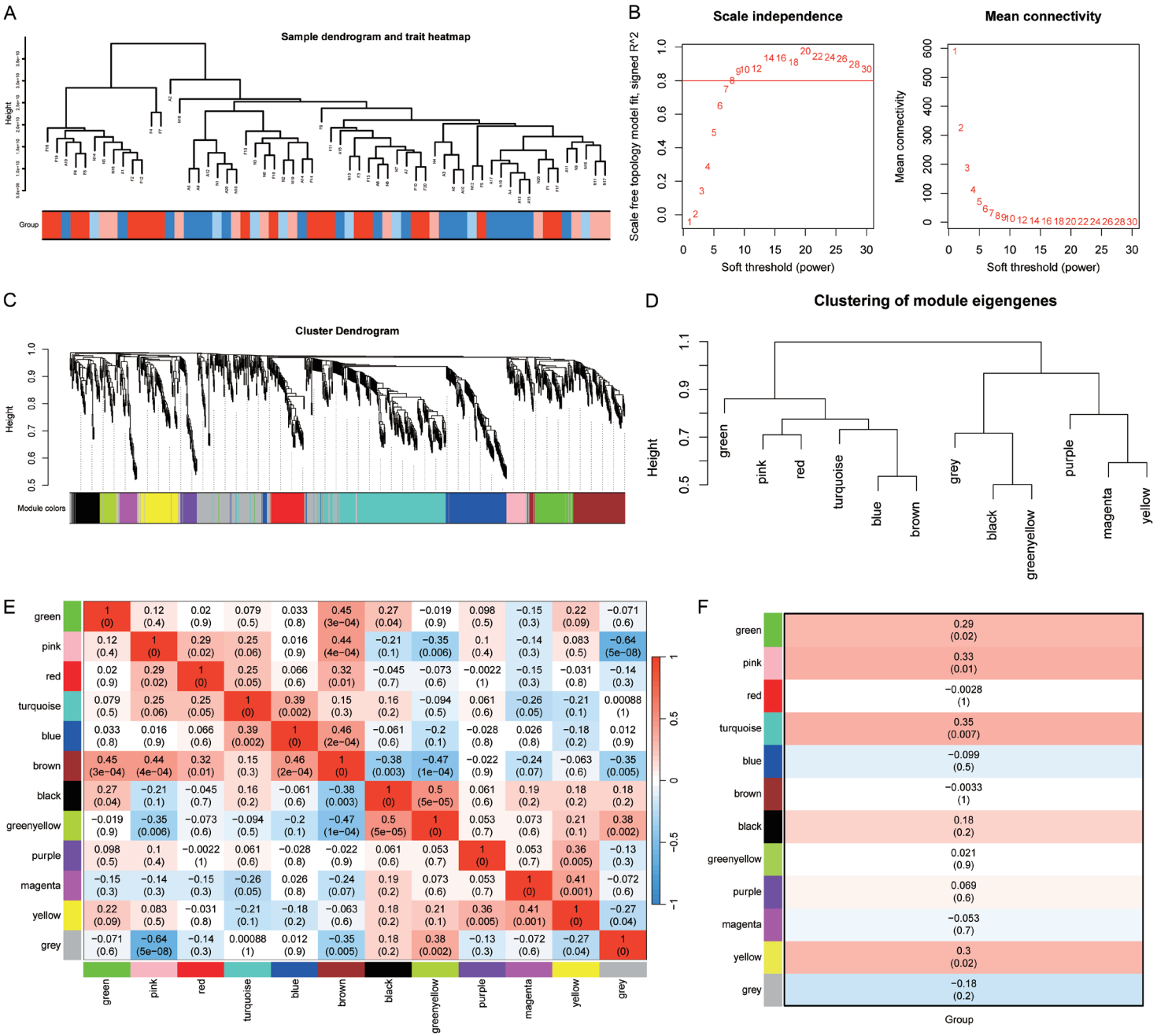
A
Sample dendrogram and trait heatmap
Height
Group
B
Scale independence
Scale free topology model fit, signed R^2
Soft threshold (power)
Mean connectivity
Mean connectivity
Soft threshold (power)
C
Cluster Dendrogram
Height
Module colors
D
Clustering of module eigengenes
Height
green
pink
red
turquoise
blue
brown
grey
black
greenyellow
purple
magenta
yellow
E
green 1 (0) 0.12 (0.4) 0.02 (0.9) 0.079 (0.5) 0.033 (0.8) 0.45 (3e−04) 0.27 (0.04) −0.019 (0.9) 0.098 (0.5) −0.15 (0.3) 0.22 (0.09) −0.071 (0.6)
pink 0.12 (0.4) 1 (0) 0.29 (0.02) 0.25 (0.06) 0.016 (0.9) 0.44 (4e−04) −0.21 (0.1) −0.35 (0.006) 0.1 (0.4) −0.14 (0.3) 0.083 (0.5) −0.64 (5e−08)
red 0.02 (0.9) 0.29 (0.02) 1 (0) 0.25 (0.05) 0.066 (0.6) 0.32 (0.01) −0.045 (0.7) −0.073 (0.6) −0.0022 (1) −0.15 (0.3) −0.031 (0.8) −0.14 (0.3)
turquoise 0.079 (0.5) 0.25 (0.06) 0.25 (0.05) 1 (0) 0.39 (0.002) 0.15 (0.3) 0.16 (0.2) −0.094 (0.5) 0.061 (0.6) −0.26 (0.05) −0.21 (0.1) 0.00088 (1)
blue 0.033 (0.8) 0.016 (0.9) 0.066 (0.6) 0.39 (0.002) 1 (0) 0.46 (2e−04) −0.061 (0.6) −0.2 (0.1) −0.028 (0.8) 0.026 (0.8) −0.18 (0.2) 0.012 (0.9)
brown 0.45 (3e−04) 0.44 (4e−04) 0.32 (0.01) 0.15 (0.3) 0.46 (2e−04) 1 (0) −0.38 (0.003) −0.47 (1e−04) −0.022 (0.9) −0.24 (0.07) −0.063 (0.6) −0.35 (0.005)
black 0.27 (0.04) −0.21 (0.1) −0.045 (0.7) 0.16 (0.2) −0.061 (0.6) −0.38 (0.003) 1 (0) 0.5 (5e−05) 0.061 (0.6) 0.19 (0.2) 0.18 (0.2) 0.18 (0.2)
greenyellow −0.019 (0.9) −0.35 (0.006) −0.073 (0.6) −0.094 (0.5) −0.2 (0.1) −0.47 (1e−04) 0.5 (5e−05) 1 (0) 0.053 (0.7) 0.073 (0.6) 0.21 (0.1) 0.38 (0.002)
purple 0.098 (0.5) 0.1 (0.4) −0.0022 (1) 0.061 (0.6) −0.028 (0.8) −0.022 (0.9) 0.061 (0.6) 0.053 (0.7) 1 (0) 0.053 (0.7) 0.36 (0.005) −0.13 (0.3)
magenta −0.15 (0.3) −0.14 (0.3) −0.15 (0.3) −0.26 (0.05) 0.026 (0.8) −0.24 (0.07) 0.19 (0.2) 0.073 (0.6) 0.053 (0.7) 1 (0) 0.41 (0.001) −0.072 (0.6)
yellow 0.22 (0.09) 0.083 (0.5) −0.031 (0.8) −0.21 (0.1) −0.18 (0.2) −0.063 (0.6) 0.18 (0.2) 0.21 (0.1) 0.36 (0.005) 0.41 (0.001) 1 (0) −0.27 (0.04)
grey −0.071 (0.6) −0.64 (5e−08) −0.14 (0.3) 0.00088 (1) 0.012 (0.9) −0.35 (0.005) 0.18 (0.2) 0.38 (0.002) −0.13 (0.3) −0.072 (0.6) −0.27 (0.04) 1 (0)
F
green 0.29 (0.02)
pink 0.33 (0.01)
red −0.0028 (1)
turquoise 0.35 (0.007)
blue −0.099 (0.5)
brown −0.0033 (1)
black 0.18 (0.2)
greenyellow 0.021 (0.9)
purple 0.069 (0.6)
magenta −0.053 (0.7)
yellow 0.3 (0.02)
grey −0.18 (0.2)
Group

Figure 5. Weighted gene co-expression network analysis (WGCNA) workflow. A: WGCNA depicting critical modules linked to anal fistula development. Outlier detection through sample clustering; B: Soft-threshold power determination using the scale-free topology model (left) and mean connectivity (right); C: Cluster dendrogram and module assignment for metabolites; D: Clustering of all identified modules; E: Heat map illustrating inter-module relationships; F: Heat map displaying module-group relationships. WGCNA: Weighted Gene Co-expression Network Analysis.

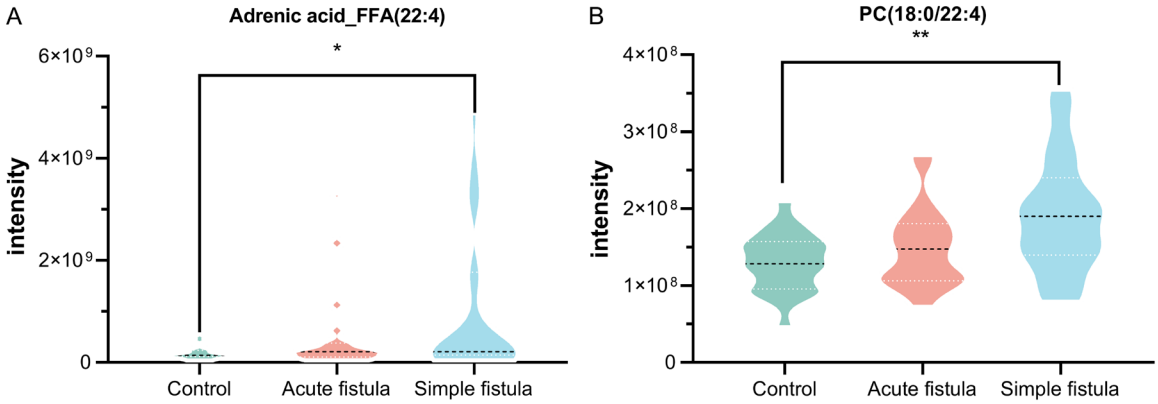

Figure 6. Concentration differences of two metabolites. (A) Adrenic acid (22:4n-6) and (B) PC (18:0/22:4) levels in healthy controls, acute anal fistula, and simple anal fistula groups. *P<0.05, **P<0.01.

fistula group. These observations were consistent with the trends observed for PC (18:0/22:4), which contains adrenic acid, across the three groups (**Figure 6A**, **6B**).

Discussion

Long-chain saturated fatty acids (LCSFAs) are known to influence the composition and function of cell membranes, which can affect the body's immune response and susceptibility to infection [18]. One potential mechanism by which LCSFAs contributes to perianal infectious diseases is through their effect on inflammation. LCSFAs are known to promote inflammatory processes, potentially exacerbating conditions that lead to infection. For instance, the consumption of LCSFAs has been linked to increased levels of pro-inflammatory cytokines, which are involved in the development of various inflammatory diseases [19]. Additionally, LCSFAs can influence gut microbiota, which is vital for maintaining intestinal health and preventing infection. High LCSFA intake could lead to dysbiosis, a condition characterized by an imbalance in the microbial community, which has been associated with an increased susceptibility to infection [20]. Additionally, LCSFAs affect the integrity of the intestinal barrier. A compromised intestinal barrier can allow pathogens to penetrate the gut lining, leading to infection. Studies have shown that maintaining adequate levels of saturated fatty acids in the intestine can help stabilize the gut barrier and reduce the risk of infection [21]. Furthermore, the antibacterial properties of LCSFAs have been explored, with some studies suggesting that they can inhibit the growth of certain bacteria. However, the effectiveness of LCSFAs as antibacterial agents is influenced by their solubility and the conditions of the medium in which they are used. Enhancing the solubility of LCSFAs may improve their antibacterial efficacy, possibly offering a natural alternative for preventing infection [22].

Amino acids play a crucial role in the management and treatment of perianal infectious diseases, primarily through their support for tissue repair and immune function [23]. These essential compounds are involved in various metabolic pathways that are critical for maintaining tissue integrity and enhancing the body's immune response. For instance, amino acids such as glutamine and arginine influence immune cell function and have been studied for their roles in infection and tissue repair processes [24, 25]. In addition to their immune-supportive roles, amino acids are vital for tissue repair. They provide the necessary building blocks for protein synthesis, essential for the regeneration of damaged tissues. This is par-

ticularly important for perianal diseases, where maintaining the integrity of the mucosal barrier is crucial for preventing further infection and promoting healing [26].

The relationship between fatty acid β-oxidation and anal fistula, particularly in the context of obesity, is an intriguing area of study. Obesity is known to influence various metabolic pathways, including fatty acid metabolism, which may have implications for the development and progression of anal fistulas [27]. One study highlights the role of amino acid and lipid metabolism in distinguishing Crohn's disease from idiopathic/cryptoglandular perianal fistulas [28]. Furthermore, a retrospective cross-sectional survey explored the epidemiologic profile of anal fistulas and anorectal abscess, identifying BMI as a significant factor. The study found that individuals with overweight or obesity were more prone to develop anal fistula and anorectal abscess [29].

The role of adipose tissue in anal fistula treatment has been explored, particularly through the use of adipose-derived stem cells [30]. These cells, which are influenced by fatty acid metabolism, have shown promise in treating complex perianal fistulas, suggesting a potential therapeutic avenue that leverages the metabolic characteristics of adipose tissue [31]. Moreover, a study on the long-term outcomes of fistula treatment using the LIFT-plug technique, which involves bioprosthetic materials, suggests that metabolic factors, including those related to obesity, may influence healing rates and outcomes. This highlights the importance of considering metabolic health in managing anal fistulas [32]. The relationship between obesity and anal fistula is further supported by research indicating that overweight and obesity are risk factors for anal fistula and anorectal abscesses. This suggests that metabolic dysregulation associated with obesity, such as impaired fatty acid β-oxidation, could contribute to the pathophysiology of anal fistulas [33].

Acetylcarnitine, a derivative of the amino acid L-carnitine, is known for its role in cellular energy production and its potential therapeutic effects in various medical conditions [34]. Its relevance to perianal infectious diseases, such as anal fistula, can be explored through the lens of metabolic and inflammatory pathways [35]. Anal fistulas are abnormal connections between the epithelialized surface of the anal canal and the perianal skin, often resulting from infection or inflammation [36]. The pathogenesis of anal fistulas involves complex interactions between microbiological, immunological, and genetic factors, which can be influenced by metabolic processes.

Recent studies have highlighted the metabolic distinctions between Crohn's disease-associated perianal fistulas and idiopathic or cryptoglandular perianal fistulas. These distinctions are evident in the differences in amino acid and lipid metabolism, which may offer insights into the underlying pathogenesis of these conditions [27]. Acetylcarnitine, a compound in lipid metabolism, may play a role in modulating these metabolic pathways, influencing the course of perianal diseases. Moreover, the management of perianal fistulas, particularly those associated with Crohn's disease, often involves addressing the inflammatory and infectious components. The use of biologic therapies, such as anti-TNF-α agents, has been explored for their effects on the bacteriological profile of perianal lesions, although these therapies do not significantly alter the types of microorganisms isolated from such lesions [33]. The integration of metabolic modulators like acetylcarnitine could enhance recovery and reduce postoperative complications by supporting cellular energy metabolism and reducing oxidative stress [31]. Furthermore, mesenchymal stem cells (MSCs) have been investigated for the treatment of complex perianal fistulas, with MSCs showing promising efficacy in promoting fistula closure and reducing recurrence rates. Acetylcarnitine may support MSC therapy by enhancing cellular energy production and reducing inflammation, thus improving the overall therapeutic outcome [8].

While this study provides valuable insight into the metabolic alterations associated with anal fistula, several limitations should be acknowledged. First, the sample size was relatively small, which may limit the generalizability of the findings. Future studies with larger cohorts are needed to validate these results. Second, the study focused on serum metabolomics, but additional analyses of tissue samples or gut microbiota could provide a more comprehensive understanding of the disease mechanisms. Third, the cross-sectional design of the

study limited our ability to establish causal relationships between metabolic changes and disease progression. Longitudinal studies are necessary to explore these relationships further. Finally, while we identified potential biomarkers and metabolic pathways, their clinical utility needs to be validated by prospective studies.

Future research should focus on integrating metabolomic data with other omics approaches (e.g., genomics, proteomics) to gain a more holistic understanding of anal fistula pathogenesis. Additionally, the development of targeted therapies based on the identified metabolic pathways, such as fatty acid and sphingolipid metabolism, could be exploredby preclinical and clinical trials. Finally, the use of metabolomic profiling for personalized treatment strategies in anal fistula patients warrants further investigation.

Conclusion

Patients with anal fistula undergo significant metabolic alterations, particularly in fatty acid metabolism, sphingolipid metabolism, and amino acid metabolism. Key metabolites such as adrenic acid, LysoPC (22:5n6), and PC (18:0/22:4) are associated with the progression of anal fistula, suggesting their use as biomarkers for the condition. These findings provide new insight into the metabolic underpinnings of anal fistula and suggest targets for therapeutic intervention. By integrating metabolomic profiling with traditional diagnostic approaches, this study paves the way for more personalized and effective treatment strategies for anal fistula.

Disclosure of conflict of interest

None.

Address correspondence to: Yongqing Cao, Department of Anal and Intestinal Disease, Longhua Hospital, Shanghai University of Traditional Chinese Medicine, No. 725, South Wanping Road, Shanghai 200030, China. E-mail: cyq88tcm@163.com

References

[1] Meinero P and Mori L. Video-assisted anal fistula treatment (VAAFT): a novel sphincter-saving procedure for treating complex anal fistulas. Tech Coloproctol 2011; 15: 417-422.

[2] Schwandner O. Stem cell therapy for complex anal fistula in Crohn's disease: current evidence and future perspectives. Zentralbl Chir 2023; 148: 220-227.

[3] Cheng F, Huang Z and Li Z. Efficacy and safety of mesenchymal stem cells in treatment of complex perianal fistulas: a meta-analysis. Stem Cells Int 2020; 2020: 8816737.

[4] Ratto C, Litta F, Parello A, Donisi L, Zaccone G and De Simone V. Gore bio-a® fistula plug: a new sphincter-sparing procedure for complex anal fistula. Colorectal Dis 2012; 14: e264-269.

[5] Brochard C, Siproudhis L, Fathallah N, Zerbib P, Sabbagh C, Bouchard D, Etienney I and Cotte E. Allogenic stem cells in anal fistulas of Crohn's disease: from promising premises to real life experience. Inflamm Bowel Dis 2025; 31: 671-676.

[6] Mitchel EB and Rosh JR. Pediatric management of Crohn's disease. Gastroenterol Clin North Am 2022; 51: 401-424.

[7] Wang JP, Cai C, Du JL, Shi HQ, Liu QW, Dai ZH and Zhong ZF. Role of interleukin-17 in the pathogenesis of perianal abscess and anal fistula: a clinical study on 50 patients with perianal abscess. ANZ J Surg 2019; 89: 244-247.

[8] Wang H, Jiang HY, Zhang YX, Jin HY, Fei BY and Jiang JL. Mesenchymal stem cells transplantation for perianal fistulas: a systematic review and meta-analysis of clinical trials. Stem Cell Res Ther 2023; 14: 103.

[9] Scharl M, Weber A, Fürst A, Farkas S, Jehle E, Pesch T, Kellermeier S, Fried M and Rogler G. Potential role for SNAIL family transcription factors in the etiology of Crohn's disease-associated fistulae. Inflamm Bowel Dis 2011; 17: 1907-1916.

[10] McCurdy JD, Parlow S, Dawkins Y, Samji K, Rhee GG, Oliveira L, Macdonald B, Sabri E and Murthy S. Tumor necrosis factor inhibitors may have limited efficacy for complex perianal fistulas without luminal Crohn's disease. Dig Dis Sci 2020; 65: 1784-1789.

[11] Kmieć Z, Cyman M and Ślebioda TJ. Cells of the innate and adaptive immunity and their interactions in inflammatory bowel disease. Adv Med Sci 2017; 62: 1-16.

[12] Vogel JD, Johnson EK, Morris AM, Paquette IM, Saclarides TJ, Feingold DL and Steele SR. Clinical practice guideline for the management of anorectal abscess, fistula-in-ano, and rectovaginal fistula. Dis Colon Rectum 2016; 59: 1117-1133.

[13] Bartel J, Krumsiek J and Theis FJ. Statistical methods for the analysis of high-throughput metabolomics data. Comput Struct Biotechnol J 2013; 4: e201301009.

[14] Vinaixa M, Samino S, Saez I, Duran J, Guinovart JJ and Yanes O. A guideline to univariate statistical analysis for LC/MS-based untargeted metabolomics-derived data. Metabolites 2012; 2: 775-795.
[15] Ewald JD, Zhou G, Lu Y, Kolic J, Ellis C, Johnson JD, Macdonald PE and Xia J. Web-based multiomics integration using the analyst software suite. Nat Protoc 2024; 19: 1467-1497.
[16] Pang Z, Lu Y, Zhou G, Hui F, Xu L, Viau C, Spigelman AF, MacDonald PE, Wishart DS, Li S and Xia J. MetaboAnalyst 6.0: towards a unified platform for metabolomics data processing, analysis and interpretation. Nucleic Acids Res 2024; 52: W398-W406.
[17] Langfelder P and Horvath S. WGCNA: an R package for weighted correlation network analysis. BMC Bioinformatics 2008; 9: 559.
[18] Arellano H, Nardello-Rataj V, Szunerits S, Boukherroub R and Fameau AL. Saturated long chain fatty acids as possible natural alternative antibacterial agents: opportunities and challenges. Adv Colloid Interface Sci 2023; 318: 102952.
[19] Jenab A, Roghanian R and Emtiazi G. Bacterial natural compounds with anti-inflammatory and immunomodulatory properties (mini review). Drug Des Devel Ther 2020; 14: 3787-3801.
[20] Chen P, Torralba M, Tan J, Embree M, Zengler K, Stärkel P, van Pijkeren JP, DePew J, Loomba R, Ho SB, Bajaj JS, Mutlu EA, Keshavarzian A, Tsukamoto H, Nelson KE, Fouts DE and Schnabl B. Supplementation of saturated long-chain fatty acids maintains intestinal eubiosis and reduces ethanol-induced liver injury in mice. Gastroenterology 2015; 148: 203-214, e16.
[21] Arellano H, Nardello-Rataj V, Szunerits S, Boukherroub R and Fameau AL. Saturated long chain fatty acids as possible natural alternative antibacterial agents: opportunities and challenges. Adv Colloid Interface Sci 2023; 318: 102952.
[22] Crowther RR and Qualls JE. Metabolic regulation of immune responses to mycobacterium tuberculosis: a spotlight on L-arginine and L-tryptophan metabolism. Front Immunol 2021; 11: 628432.
[23] Moore B, Mahoney K, Zeng MF, Djuricanin P and Momose T. Ultraviolet photodissociation of proteinogenic amino acids. J Am Chem Soc 2023; 145: 11045-11055.
[24] Zhang Z, Wang Y, Xia L and Zhang Y. Roles of critical amino acids metabolism in the interactions between intracellular bacterial infection and macrophage function. Curr Microbiol 2024; 81: 280.
[25] Yang Y, Li W, Sun Y, Han F, Hu CA and Wu Z. Amino acid deprivation disrupts barrier function and induces protective autophagy in intestinal porcine epithelial cells. Amino Acids 2015; 47: 2177-2184.
[26] Adegbola SO, Sarafian M, Sahnan K, Ding NS, Faiz OD, Warusavitarne J, Phillips RKS, Tozer PJ, Holmes E and Hart AL. Differences in amino acid and lipid metabolism distinguish Crohn's from idiopathic/cryptoglandular perianal fistulas by tissue metabonomic profiling and may offer clues to underlying pathogenesis. Eur J Gastroenterol Hepatol 2021; 33: 1469-1479.
[27] Marx W, Lane M, Hockey M, Aslam H, Berk M, Walder K, Borsini A, Firth J, Pariante CM, Berding K, Cryan JF, Clarke G, Craig JM, Su KP, Mischoulon D, Gomez-Pinilla F, Foster JA, Cani PD, Thuret S, Staudacher HM, Sánchez-Villegas A, Arshad H, Akbaraly T, O'Neil A, Segasby T and Jacka FN. Diet and depression: exploring the biological mechanisms of action. Mol Psychiatry 2021; 26: 134-150.
[28] Kushwaha V, Rai P, Varshney S, Gupta S, Khandelwal N, Kumar D and Nilkanth Gaikwad A. Sodium butyrate reduces endoplasmic reticulum stress by modulating CHOP and empowers favorable anti-inflammatory adipose tissue immune-metabolism in HFD fed mice model of obesity. Food Chem (Oxf) 2022; 4: 100079.
[29] Ye S, Huang Z, Zheng L, Shi Y, Zhi C, Liu N and Cheng Y. Restricted cubic spline model analysis of the association between anal fistula and anorectal abscess incidence and body mass index. Front Surg 2024; 10: 1329557.
[30] Topal U, Eray IC, Rencüzoğulları A, Yalav O and Alabaz Ö. Short-term results of adipose-derived stem cell therapy for the treatment of complex perianal fistula a single center experience. Ann Ital Chir 2019; 90: 583-589.
[31] Garcia-Arranz M, Garcia-Olmo D, Herreros MD, Gracia-Solana J, Guadalajara H, de la Portilla F, Baixauli J, Garcia-Garcia J, Ramirez JM, Sanchez-Guijo F and Prosper F; FISPAC Collaborative Group. Autologous adipose-derived stem cells for the treatment of complex cryptoglandular perianal fistula: a randomized clinical trial with long-term follow-up. Stem Cells Transl Med 2020; 9: 295-301.
[32] Zhao B, Wang Z, Han J, Zheng Y, Cui J and Yu S. Long-term outcomes of ligation of the intersphincteric fistula tract plus bioprosthetic anal fistula plug (LIFT-plug) in the treatment of trans-sphincteric perianal fistula. Med Sci Monit 2019; 25: 1350-1354.
[33] Gruszecka J and Filip R. Does anti-TNF-α therapy affect the bacteriological profile of specimens collected from perianal lesions? A retro-

spective analysis in patients with Crohn's disease. Int J Environ Res Public Health 2022; 19: 2892.
[34] Chiechio S, Canonico PL and Grilli M. l-acetylcarnitine: a mechanistically distinctive and potentially rapid-acting antidepressant drug. Int J Mol Sci 2017; 19: 11.
[35] Peedicayil J. L-Acetylcarnitine as a histone acetylation modulator in psychiatric disorders. Psychopharmacology (Berl) 2018; 235: 3361-3362.
[36] Leńska-Mieciek M, Madetko-Alster N, Alster P, Królicki L, Fiszer U and Koziorowski D. Inflammation in multiple system atrophy. Front Immunol 2023; 14: 1214677.